

Finite Element Modeling and Optimization of Estimated Cutting Forces during Machining of Inconel 718

Khalaf Nasralla², Suha K. Shihab¹, Adel K .Mahmoud²

1Department of Materials Engineering, college of Engineering, University of Diyala, Iraq

2Department of Mechanical Department, college of Engineering, University of Diyala, Iraq

Abstract

In this study, the effect of different cutting parameters (cutting speed, feed rate, and depth of cut) on cutting force under dry hard turning of Inconel 718 was investigated. 3D- Finite element modeling of orthogonal machining based Taguchi L₉ design was used to obtain the results. The obtained results of simulation were verified with previous study and it was showed a good agreement. The effects of feed rate, cutting speed and depth of cut on cutting force were analyzed based on. Analysis of Variance (ANOVA) was performed to understand the percentage influence of all the cutting parameters. The Taguchi L₉ orthogonal array was selected to determine optimal values of cutting parameters. The results showed that the cutting force increases significantly with increase of depth of cut.

Keywords - Inconel 718, Cutting force, 3D modeling, Taguchi design, ANOVA, Optimization

I. INTRODUCTION

Inconel 718 (a nickel based superalloy) is widely used in the aerospace industry for the manufacture of aero engine components that are subjected to relatively high temperature and stresses during operation, such as turbine disks, shafts, compressor blades and combustion chamber casings and marine applications because of its high strength to weight ratio, mechanical, thermal shock and fatigue and high corrosion resistance. Alloy 718 (Inconel) is an austenitic nickel-base superalloy which is used in applications requiring high strength to approximately 760°C and oxidation resistance to approximately (982°C). [1-3]. Many researchers have been working to understand the relation between cutting parameter and generated cutting force during turning process. Sulaiman S. et al (2013) studied the distribution of cutting force during high speed machining of AISI 4340 steel using FEM based on the ABAQUS/explicit which includes Johnson-Cook material model (JC). They found that the cutting forces have a decreasing trend as rake angle increased to positive direction [4]. Yash R. Bhoyar and Kamble

(2013) constructed a model using finite element analysis of orthogonal cutting of AISI 1040 carbon steel to find the cutting forces taking place at many points through the chip-tool contact district and the coating-substrate boundary for the given cutting tool materials. Their result indicated that the cutting force is an imperative variable in the generation of temperature at machined surface and with increase the value of rake angle caused the decrease of the cutting force[5]. Rao. C. J.et al (2013) studied the influence of cutting parameters on cutting force during machining AISI 1050 steel with made of ceramic tool. Taguchi method was used for the experiments to analysis of variance. Their result demonstrated that depth of cut has a significant influence on cutting force [6]. Franci Pusavec (2014) applied response surface methodology (RSM) for optimization machining conditions (dry, near-dry (MQL), cryogenic and cryo-lubrication) for Inconel 718 alloy. Cutting forces were measured, analyzed and modeled. The results showed that the cooling/lubrication condition has an influence in reducing cutting forces of machining process [7]. Jagadesh T and Samuel G (2014) performed 3D modeling of finite element analysis for calculation of cutting forces during micro-turning of Ti6Al4V alloy by coated carbide insert (TiN-AlTiN). They used Johnson- Cook material model to represent the flow stress of the material. They detected that when cutting speed increases, there was decrease in the cutting force due to the effect of thermal softening [8]. Mane, S. and Kumar, S. et al. (2019) studied an analysis of cutting force and optimization of cutting parameters during the turning of hardened AISI 4140 alloy steel using TiAlN-TiN coated insert. Their result showed that cutting speed has prominent effect on the measured cutting forces. [9].Ye Li and Chunbin Cai(2016) investigated the effect of back angle, tool rake angle, and feed cutting speed on cutting force by varying cutting parameters during machining of nickel-based superalloy with PCBN GH4169 tool. They used finite element simulation to establish two dimensional cutting simulation model of superalloy. Their results showed that the increase of the

feed rate, the cutting force increases almost linearly while cutting speed slightly reduces the cutting force [10]. Lianjie Ma et al. (2017) examined the influence of cutting parameters on cutting force using finite element analysis of machining of composite material (Fluorosilicic mica glass ceramics). The results appeared that the constitutive model fit reflects the cutting removal process of fragile material. Also, the results of simulation were well agreed with theoretical data and experimental data. The effects of cutting depth and feed speed on cutting force were larger than those of tool cutting edge angle and cutting speed [11]. Ganesh. S. Sonawane (2017) carried out an experimental research on distribution of cutting forces of super alloy Inconel 718 during high speed turning using two grades of ceramic inserts (KYS25 and KYS30) with three various nose radii. The result confirmed that using tool insert type KYS30 shape leads to good quality of surface and lesser cutting forces [12]. Anil K. Srivastava et al.(2017) expected the cutting forces during high speed machining of Ti-6Al-4V alloy using super-finished of cutting edge inserts. The cutting forces are expected perfectly using 2D finite element model using ABAQUS software. The results indicated that the expected cutting forces using FE simulation agree well with the measured forces. In addition, the predicted thrust force was less than 7%, which can be improved with the accurateness of considered shear angle [13]. Taric (2017) et al. investigated the cutting forces during turning of EN 90MnCrV8 steel using two types of inserts HM and CBN. The results illustrated that the vary of the cutting force against time is more significant for HM than for CBN insert where values are considerably lower [14]. Asit Kumar Parida and Kalipada Maity (2018) studied the effect of thermally assisted turning on three nickel base alloys (Inconel 718, Inconel 625 and Monel-400) using flame heating. Cutting force has been determined in both room and hot temperature conditions (300 C and 600 C). They noticed that there was significant decrease of cutting force for all three used nickel alloys in hot turning compared to machining at room temperature [15]. Zeqiri F(2018) studied the effects of parameters of cutting process on cutting forces based on Taguchi method. The used material was Inconel 625 for two cases with both heat treatment and without heat treatment using cutting coated carbide tool. Their results showed with the increase of cutting speed was caused decrease in the values cutting force and with the increase of cutting feed, cutting forces increase [16]. Xu Zhang (2018) investigated the machinability of Titanium alloy (TC21) during 3D finite element model of oblique machining process. It was obtained that the simulation results were agreed with the trials and it was observed that the cutting forces decrease with the increasing of rake angle [17].

The aim of this research is investigating the effect cutting parameters i.e. (cutting speed, feed rate, and depth of cut) on cutting force under dry hard turning process of Inconel 718 using 3D FE simulations based ABAQUS/explicit for orthogonal machining turning processes. Also the validation of obtained simulation data results was achieved by modeling the results of previous experimental study used in reference [15]. Then design of experimental (DOE) based Taguchi L_9 design was used to obtain optimal cutting parameters.

II. FINITE ELEMENT MODELING OF TURNING PROCESS

Finite element analysis is a most beneficial method for the definition of variables in machining processes and it has been successfully utilized for metal machining simulations due to an agreeable of simulation results with measurements of process attributes. The current study is based on the implementation of finite element simulation for turning process. Once the model expanded for determination cutting force for turning operation, it can also be employed for other machining processes like milling, drilling and grinding.

In simulation of orthogonal cutting, the response cutting force is obtained due to the elastic and plastic deformation as well as friction force [1,5]. Produced cutting forces during cutting process have a immediate influence on generation of heat and consequently on accuracy and quality of machined surface and tool wear. The data of cutting forces for different cutting parameters assists the designer and manufacturer for rising the effectiveness of machine tools. The cutting forces effected by geometry of cutting tool, material of workpiece, cutting speed, depth of cut and feed rate. Therefore, in present work the magnitude of cutting force on the reference point of cutting tool was determined using FE modelings based on Taguchi design to search out optimal values of cutting parameters that generate lowest cutting force in turning process. The analyses are carried out using FEM/Abaqus (Dynamic explicit) software where it allows dealing with complex material models that include high plastic deformation like machining process. A nine models on the base of Taguchi design were made to estimate the effect of parameters on the cutting force during turning of Inconel718 with coated carbide insert. The constitutive models were suggested using Johnson - Cook. Friction coefficient between cutting tool and workpiece (and chip) is taken as 0.3μ . Fig. 1 shows the sequence of the steps of 3D ALE dynamic explicit modelling for both workpiece and cutting tool.

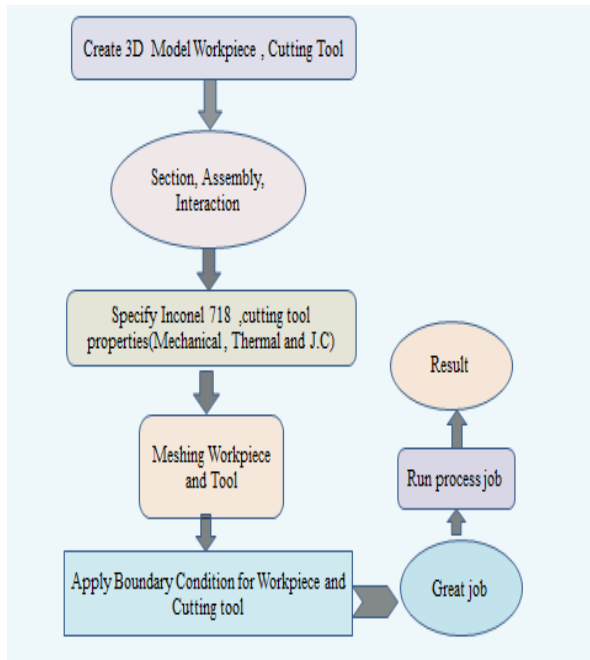


Fig .1 Sequence of the steps of 3D ALE dynamic explicit modelling for both workpiece and cutting tool.

A. Boundary conditions

Model geometries for the workpiece and cutting tool insert were defined. Appropriate boundary conditions were applied to constrain the movement of the side and bottom faces of the workpiece as shown in the perspective Fig.2. Additionally, the cutting tool was constrained to move only in the x-direction and the boundary conditions applied in reference point. Also, new boundary condition has been used in each run input for the nine models due to changing of the cutting parameters i.e. speed, feed and depth of cut. Subsequently, the adaptive Langrangian Eulerian (ALE) formulation, mesh smoothing approach and thermo mechanical coupling were also defined. The workpiece was divided to many portions to reduce running time during simulation.

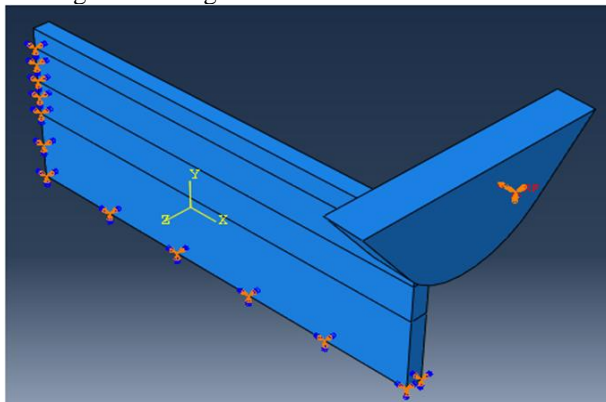


Fig 2. Boundary conditions on workpiece and cutting tool

B. Tool Modelling

The tool geometry has a great influence on the cutting force on the machined workpiece, so it has been given a very keen importance in the model to design to tool geometry. In the Abaqus 3D analysis, cutting tool is assumed to be a rigid body with reference point. Table 1 reveals the geometric variables of the selected coated PVD tool. While the thermal and mechanical properties of cutting tool are given in Table 2. Finite element mesh of tool was modelled using 45 elements approximate global size (8µm). Hex- elements shape is used for the analysis. The distribution of mesh on the radius of cutting tool is finer to make the curve smoother and more accurate as shown in Fig.3. The mesh density just on the cutting plane is very fine this is intentionally done to increase the accuracy of the result in this zone. The used Element type was (CED8R) with 8 nodes hexahedron coupled with reduced integration and hourglass control which are suitable for explicit dynamics analyses.

sample	C	S	P	AL	Cu	Co	Fe	Mn
%	0.034	0.011	0.007	0.497	0.033	0.159	17.22	0.093
sample	Cr	V	Ti	Mo	Nb	W	Si	Ni
%	17.38	0.092	0.885	2.86	5.57	0.065	0.177	53.446

Table 1: Geometric variables of the tool

Rake Angle, α	7°
Noise radius (mm)	1.2
Type of coating	PVD

Table 2: Thermal and mechanical properties of cutting tool [18,19,20]

Elastic Modulus, E (GPa)	800
Poisson's Ratio	0.2
Thermal Expansion (mm/mm * °C)	4.7*10 ⁻⁶
Thermal Conductivity (W/m*°C)	47
Density(kg/m ³)	15000
Specific heat (J/kg)	203

C. Workpiece Modelling

In this study, the used workpiece material was Inconel718 alloy with the dimension of (6mm Length*2mmWidth). The mechanical, physical and thermal properties of the workpiece material are presented in Table 3 while Table 4 shows the chemical composition of the workpiece material that used in this study. The used element type is C3D8RT with 8 nodes hex, temperature displacement coupled element. ALE

adaptive meshing combined with pure Langrangian boundary condition was implemented to mesh the workpiece material domain with 4500 elements and global size (0.02μm). This element number was changed in every run of nine models due to the difference in the values of depth and feed. Fig. 3 represents the meshing for the finite element model.

Table3 Mechanical, Physical and Thermal Properties of Inconel718 alloys at room temperature[18-20].

Property	
Yield strength (MPa)	1310
Elastic modulus (GPa)	206
Ultimate tensile stress (MPa)	1375
Elongation (%)	25
Specific heat capacity (J/Kg.°C)	430
Thermal conductivity (W/m.°C)	11.2
Coefficient of thermal expansion (10 ⁻⁶ /	14.4
Melting range (°C)	1260-1333
Density (Kg/m3)	8470

Table 4 The chemical composition of Inconel718 alloys

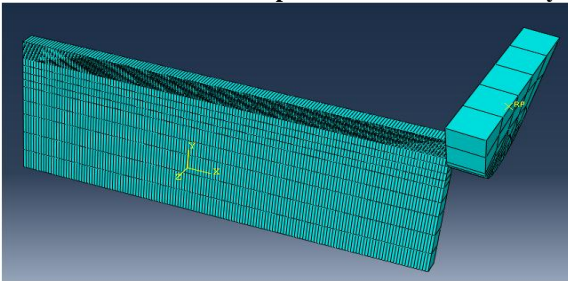


Fig 3. Meshing elements for the workpiece and cutting tool

Material Disruption of the finite element mesh is necessary for modelling chip formation, therefore besides the material model, the Johnson-Cook damage model was also applied in finite element simulation. This is a fracture model for ductile materials and consists of two phases, a damage initiation and a damage evolution phase. The Johnson-Cook damage model assumed is given in eq.(1):

$$\sigma = [A + B\epsilon^n] [1 + c \ln \frac{\dot{\epsilon}}{\dot{\epsilon}^0}] [1 - \frac{T - T^0}{T_m - T^0}]^m \dots \dots (1)$$

where: σ :flow stress; A: Yield stress constant; B :Strain hardening coefficient; C :Strain rate dependence coefficient; n :Strain hardening exponent; $\dot{\epsilon}$: True strain rate; $\dot{\epsilon}^0$: Reference true strain rate; m :Temperature dependence coefficient; T :Temperature; T_m: Melting temperature; T_r: Room temperature.

The Johnson-cook material constants of Inconel718 presented in Table 5. The value of friction coefficient between the tool and workpiece (μ) was equal to 0.3 as coulomb friction model which was selected in all simulation runs.

Table 5 Johnson-Cook material model constants for Inconel 718 [18,19,20]

A (MPa)	B (MPa)	C	n	m	Tr (°C)	T _m (°C)
1241	622	0.01	0.65	1.3	20	1297

III. TAGUCHI DESIGN

The Taguchi L₉ orthogonal array was selected to perform the simulation of cutting process. The machining controllable: cutting speed, feed rate, and depth of cut parameters were depended and their levels that were used during modelings are shown in Table 6. The L₉ orthogonal array with three columns and nine rows was suitable for use in this research. In this work, analysis based on the Taguchi method is performed by utilizing the Minitab software to estimate the significant factors of the CNC turning process parameters on cutting force in workpiece analysis of the obtained data from the simulations. Analysis of Variance (ANOVA) was performed to understand the percentage influence of all the cutting parameters. Table 7 shows the cutting parameters in Taguchi L₉ array in term arrangement. In Taguchi method, the analysis of variation is performed using Signal-to-Noise ratio (S/N). There are three S/N ratio criteria approaches of common interest for optimization as shown in Table 8. In this work, the objective is to minimize cutting force response so smaller is better was chosen for the response.

Table 6. Cutting parameters with their levels

Symbol	Machining parameters	Unite	Level 1	Level 2	Level 3
<i>v</i>	Cutting speed	m/min	60	80	100
<i>f</i>	Feed rate	mm/rev	0.05	0.15	0.25
<i>d</i>	Depth of cut	mm	0.2	0.25	0.3

Table 7. Taguchi L9 array in term of cutting parameters.

Run. no	Cutting speed(m/min)	Feed rate(mm/rev)	Depth of cut(mm)
1	60	0.05	0.2
2	60	0.15	0.25
3	60	0.25	0.3
4	80	0.05	0.3
5	80	0.15	0.2
6	80	0.25	0.25
7	100	0.05	0.25
8	100	0.15	0.3
9	100	0.25	0.2

Table8. Criteria of S/N ratio

Goal	S/N Ratio Formula
Nominal -is-best	$\frac{S}{N} = 10 \log \left[\frac{y^2}{s^2} \right]$
Larger-is-better(maximize)	$\frac{S}{N} = - 10 \log \left[\frac{1}{n} \sum \frac{1}{y_i^2} \right]$
Smaller-is-better(minimize)	$\frac{S}{N} = - 10 \log \left[\frac{1}{n} \sum y_i^2 \right]$

IV.RESULTS AND DISCUSSION

A. Validation of simulation results

The results of modelings were validated by comparing the cutting forces between the simulation results and the experimental results of the previous study [15]. The first model has been built on the base of same cutting conditions that used in the previous experimental study of the reference [15] in order to confirm the reliability of the simulation results. In this model, the input cutting parameters data were cutting speed at 100 m/min, feed rate at 0.13 mm/rev, depth of cut at 0.5 mm and heating temperature at 30 °C. Fig. 4 shows the results of the model using Abaqus dynamic explicit simulation. It can be concluded from Fig. 4 that there was good agreement between the published experimental results and simulated results for the cutting forces.

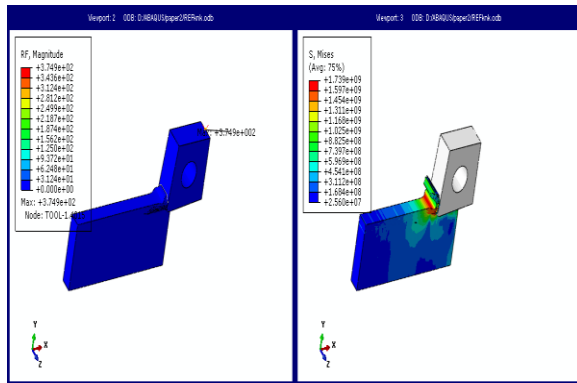


Fig 4. simulation results for validation of modeling.

B. Cutting force analysis:

Nine 3D simulation models were performed using the selected cutting parameters on the base of Taguchi L₉ design. From 3D simulations, the magnitudes of the resultant cutting force (Fc) in reference point of cutting tool were obtained as shown in Fig. 5. Then the simulation data of cutting force were analyzed depending on signal to noise ratio (S/N) and the ANOVA analysis. The cutting force must be smaller as possible to reduce the power required to operation, therefore the quality characteristic "smaller is better" was considered to study the effect of cutting parameters on the cutting force. Table 9 shows the

simulate results of workpiece cutting force along with S/N ratio.

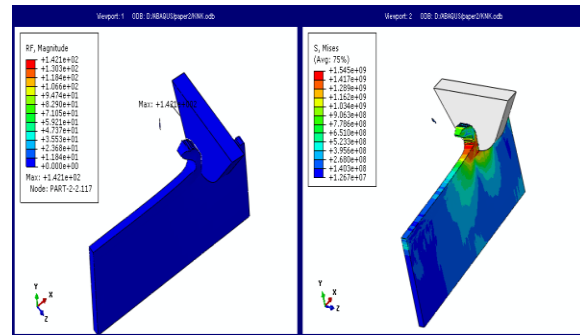


Fig. 5. Simulation results of resultant cutting forces and von Mises stresses

Table 9 Corresponding S/N ratio for the cutting force

Run.no	v(m/min)	f(mm/rev)	d(mm)	Fc(N)	S/N ratio
1	60	0.05	0.2	100	-40.0000
2	60	0.15	0.25	137	-42.7344
3	60	0.25	0.3	177	-44.9595
4	80	0.05	0.3	144	-43.7504
5	80	0.15	0.2	121	-41.6557
6	80	0.25	0.25	139	-43.4637
7	100	0.05	0.25	97	-40.9065
8	100	0.15	0.3	127	-42.0761
9	100	0.25	0.2	106	-41.2892

Fig. 6 depicts the main effect plot for S/N ratio on the cutting force. Based on the results observed in Fig 6 the optimal machining parameters that produce minimum value of cutting force are A₃B₁C₁ i.e. (cutting speed 100m/min, feed rate 0.05 mm/rev and depth of cut 0.2 mm). An increase in the depth of cut lead to increasing cutting force and the energy required. With the increase in depth of cut chip thickness become significant which causes more material to deform that requires more cutting force to cut the chip [6,7,9,11,12,16]. Further, if the feed rate increases the section of the sheared chip increases because the metal resists the rupture more and requires larger efforts for chip removal which subsequently increases the resultant cutting force[8,10,16].

Normal probability plot is represented in Fig. 7 was obtained to ensure that the data is normally fit distributed. It can be seen from Figure7 that the data points fitted lie on the straight line or are closer to line which validates the normality distribution of the simulate data. The mean S/N ratio at each level of cutting parameters was computed by taking arithmetic mean average of S/N ratio at the selected level. Table 10 shows the mean S/N ratio for all nine models. Table.11 shows the ANOVA results for cutting force and the contribution of each machining parameters. It is clear from the results of Table 10 that the depth of cut

is dominant factor affecting cutting force where its contribution is (48%).The second factors effecting cutting force is cutting speed where its contribution is (23%).While feed rate has least effect on temperature where its contribution (21%).

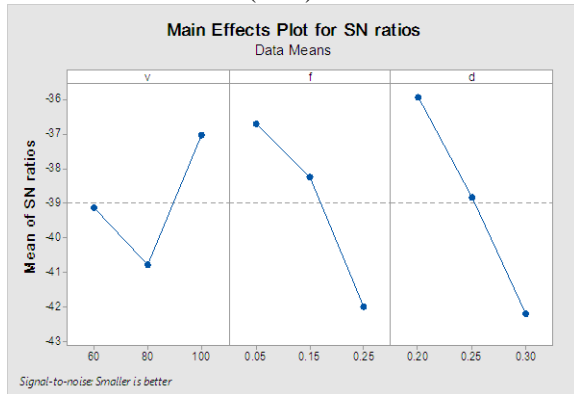


Fig. 6 Main effect plot of cutting force

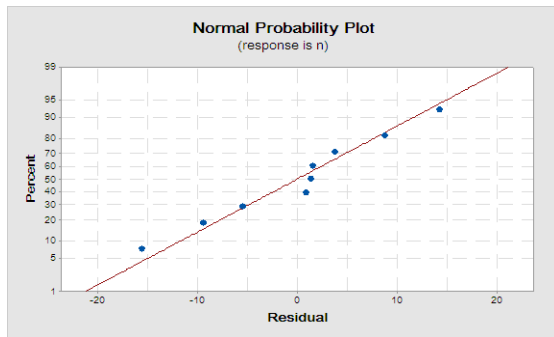


Fig. 7 Normal probability plot of cutting force

Table 10 Response table of cutting force

Cutting parameters	Level1	Level2	Level3	Max-Min	Rank
v	138.0	134.7	110	28	2
f	113.7	128.3	140.7	27	3
d	109	124.3	149.3	40.3	1

Table 11. ANOVA results for cutting force.

Factors	SS	DF	MS	F	P	Contribution % (P)
v	1176	1	1176	13.78	0.014	23%
f	1093.5	1	1093.5	12.82	0.016	21%
d	2440.2	1	2440.2	28.6	0.003	48%
Error	426.6	5	426.6			8%
Total	5136.2	8				100%

The final regression equation for cutting force F_c in term of actual factors is given by the equation (2):

$$F_c = 62.5 - 0.700 v + 135.0 f + 403.3 d \dots\dots(2)$$

Fig.8 reveals the comparison between the simulation and predicted values of cutting force which were

obtained from regression equation 2. It can be observed from Figure 8 that the predicted and simulate values are very close to each other and this refers that there is a very good relation between predicted and simulation results.

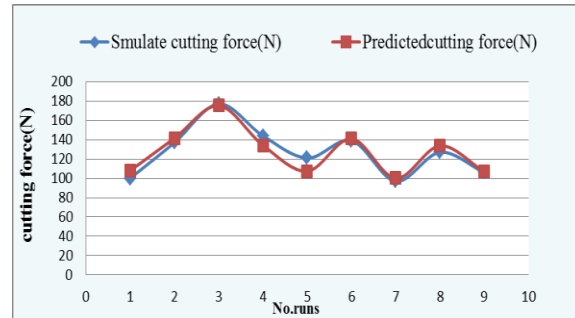


Fig.8 Comparison of simulate and predict values of cutting force

V. CONCLUSION

The main conclusions which can be deduced from this research are:

1. FEM could yield a reduction in overall machining costs and saves time through an economic analysis by applying the simulation software to predict the machining response parameters of Inconel 718 alloy.
2. There was good agreement between experiment and simulation. The average discrepancy was 10 %.
3. 3D Abaqus turning process and Johnson cook flow stress model have been used to get the near possible simulation of the cutting forces during turning of Inconel 718.
4. Cutting forces are mainly affected by depth of cut followed by cutting speed and feed rate respectively.
5. Taguchi's robust design was powerfully used for optimizing turning parameters on Inconel 718. The optimal value for cutting force was obtained from the combination of controllable machining parameters A3B1C1 (cutting speed 100 m/min, feed rate 0.05mm/rev and depth of cut 0.2 mm) which is refers to the optimum machining parameters.

REFERENCES

- [1] Chen, Y., " Prediction of Subsurface Damage During Machining Nickel-Based Superalloys" unpublished Doctor of Philosophy Thesis Submitted to, (2013) .pp. 1-25, Clemson University, USA . 2013
- [2] Samuel Rosenberg, S.J., Nickel and its alloys 'No. NBS-592'. NATIONAL BUREAU OF STANDARDS GAITHERSBURG MD., Washington, D.C. 20234,1968
- [3] Iturbe, A., Hormaetxe, E., Garay, A. and Arrazola, P.J. "Surface integrity analysis when machining inconel 718 with conventional and cryogenic cooling" Procedia CIRP, 45, pp.67-70. 2016
- [4] Sulaiman, S., Roshan, A. and Ariffin, M.K.A." Finite Element Modelling of the effect of tool rake angle on tool temperature and cutting force during high speed machining of AISI 4340 steel" In IOP Conference Series: Materials Science and Engineering (Vol. 50, No. 1, p. 012040). IOP Publishing. 2013

- [5] Bhojar, Y.R. and Kamble, P.D."Finite element analysis on temperature distribution of turning process"Int J Mod Eng Res, 3, pp.541-6. 2013
- [6] Rao, C.J., Rao, D.N. and Srihari, P." Influence of cutting parameters on cutting force and surface finish in turning operation" Procedia Engineering, 64, pp.1405-1415. 2013
- [7] Pusavec, F., Deshpande, A., Yang, S., M'Saoubi, R., Kopac, J., Dillon Jr, O.W. and Jawahir, I.S., " Sustainable machining of high temperature Nickel alloy–Inconel 718: part 1–predictive performance models"Journal of cleaner production, 81, pp.255-269. 2014
- [8] Jagadesh, T. and Samuel, G.L." Finite Element Modeling for Prediction of Cutting Forces during Micro Turning of Titanium Alloy" In 5th International & 26th All India Manufacturing Technology, Design and Research Conference (AIMTDR) December 12th–14th, IIT Guwahati, Assam, India. 2014
- [9] Mane, S. and Kumar, S. " Optimization of Cutting Parameters in Dry Turning of AISI 4140 Hardened Alloy Steel with Coated Carbide Tool" In Proceedings of International Conference on Intelligent Manufacturing and Automation (pp. 455-462). Springer, Singapore. 2019
- [10] Li, Y. and Cai, C., "Finite Element Analysis of High Temperature Alloy Cutting Process Based on Abaqus" Key Engineering Materials, 667. 2016
- [11] Ma, L., Li, C., Chen, J., Li, W., Tan, Y., Wang, C. and Zhou, Y., "Prediction model and simulation of cutting force in turning hard-brittle materials" The International Journal of Advanced Manufacturing Technology, 91(1-4), pp.165-174. 2017.
- [12] Sonawane, G. and Pawade, R., " Analysis of Cutting Forces in High Speed Turning of Inconel 718 by using Ceramic Tools" International Journal of Research and Scientific Innovation, 1(6), pp.107-112. 2014
- [13] Bell, T., Srivastava, A.K. and Zhang, X., " Investigations on turning Ti-6Al-4V titanium alloy using super-finished tool edge geometry generated by micro-machining process (MMP). Penn State College of Engineering, University Park, PA. 2011.
- [14] Taric, M., Kovac, P., Nedic, B., Rodic, D., Jesic, D "TOOL WEAR, CUTTING TEMPERATURE AND CUTTING FORCE DURING TURNING HARD STEEL" journal of production engineering, JPE Vol.20 (2-13). (2017)
- [15] Parida, A.K. and Maity, K. "Comparison the machinability of Inconel 718, Inconel 625 and Monel 400 in hot turning operation." Engineering Science and Technology, an International Journal, 21(3), pp.364-370. 2018
- [16] Zeqiri, F., Alkan, M., Kaya, B. and Toros, S., January. "Experimental Research and Mathematical Modeling of Parameters Effecting on Cutting Force and Surface Roughness in CNC Turning Process" In IOP Conference Series: Materials Science and Engineering (Vol. 295, No. 1, p. 012011). IOP Publishing. 2018,
- [17] Zhang, X. and Wu, H., "Effect of tool angle on cutting force and residual stress in the oblique cutting of TC21 alloy" The International Journal of Advanced Manufacturing Technology, pp.1-7. 2018.
- [18] SEIN LEUNG SOO "3D MODELLING WHEN HIGH SPEED END MILLING INCONEL 718 SUPERALLOY" unpublished Doctor of Philosophy Thesis Submitted to , pp.10-80, The University of Birmingham.UK(2003)
- [19] Ozel, T., Llanos, I., Soriano, J. and Arrazola, P. J " 3D finite element modelling of chip formation process for machining Inconel 718: comparison of FE software predictions" Machining Science and Technology, 15(1), pp.21-46. ., 2011
- [20] Arrazola, P.J., Kortabarria, A., Madariaga, A., Esnaola, J.A., Fernandez, E., Cappellini, C., Ulutan, D. and Özel, T., "On the machining induced residual stresses in IN718 nickel-based alloy: Experiments and predictions with finite element simulation" Simulation Modelling Practice and Theory, 41, pp.87-103. 2014